

Analyzing the Spatial Relationship between Building Volumes and Land Surface Temperature in Upper-Hill, Nairobi, Kenya

PATRICIA W. MWANGI^{1,2}

Abstract: In urban areas, temperatures are higher than rural areas at night as the impervious surfaces absorb heat during the day and release it at night. Higher energy requirements within buildings, health problems, air pollution are just a few problems associated with urban heat island effect. Increasing populations and greater demand for urban space has led to the destruction of vast vegetative cover for impervious surfaces. Remote sensing studies on surface temperatures have mainly focused on the 2 dimensional aspect of buildings, without much emphasis on 3 dimensional analyses. The main objective of this paper is to analyse the geometry of individual buildings, height, area and volume, and determine their relationship with land surface temperature. In this paper, topographical data acquired from Survey of Kenya was extracted and used to generate a 2 meter digital elevation model (DEM) to calculate building heights. DEM accuracy was carried out using ground control points (GCP) and a value of 0.24 meters was obtained. Landsat 30 meter imagery was analysed to generate land surface temperatures (LST). Temperatures of buildings within the study area had a maximum and minimum of 27.6 °C and 35.40 °C within the gridded surface. Height, area and volume regression analysis results showed they each had a negative correlation with land surface temperature with height having the highest R² value of 0.08.

1 Introduction

Transformation of the earth's surface into urban areas has modified the temperature within these areas compared to surrounding rural environments resulting to a phenomenon known as urban heat island (UHI) (ZHAO et al. 2015). Built-up densities and population are factors that affect the development of urban heat islands (UHI) with few studies considering built-up volumes and heights in urban heat studies (WU et al. 2013). Improvements in remote sensing sensor spatial resolution have enabled research in urbanization and surface temperature possible. Satellite sensors that have thermal bands such as Landsat (100 meters) and ASTER (90 meter) and are freely available, have enabled research over vast areas where fine thermal imagery may not be accessible or expensive to acquire. Land surface temperature studies are important in determining conducive environmental conditions for people to live in (WU et al. 2013).

Previous studies have examined land surface temperature in large cities, but there is need to examine changes in land surface temperature in smaller regions within the city or medium-sized cities which develop at a faster rate than other parts of the city (WU et al., 2013). Research contribution on individual buildings indicate the importance of pattern and closeness of land features as well as density and not only the surface material (ZHAO et al. 2015).

¹ Kenyatta University, Department of Spatial Planning and Urban Management, Nairobi, Kenya
E-Mail: mwangi.patricia@ku.ac.ke

² Leibniz Universität Hannover, Institut für Photogrammetrie und GeoInformation, Germany

Digital surface models derived from very high resolution data, either from stereo-satellite imagery or aerial photos provide highly detailed topographical information that provides critical data for planning or disaster management (ECKERT 2008; ALOBEID et al. 2009; EL GAROUANI et al. 2014; ALOBEID 2011). WU et al. (2013) developed a 3dimensional urban index (3DUI) in studying UHI while considering the height and vertical parameters in built-up areas where heat waves were experienced. ZHAO et al. (2015) studied the relationship between rooftop configuration from Quickbird imagery and surface temperatures from high resolution MASTER thermal data. The purpose of this research is to demonstrate the use of remote sensing in analyzing the impact the building size has with regards to land surface temperature. This research intends on analyzing land surface temperature distribution on individual buildings in the study area in relation to its physical dimensions.

2 Study Area

The study area is in Upper-Hill, Nairobi Kenya, which is 4 Km from the central business district (CBD). The study area covers approximately 4 Km². The area was selected due to its rapid development as businesses choose locations where there is less traffic congestion, ample parking space and better access. Ground coverage ratio within the study area has increased to 35-60% and plot ratio of 150-300% leading to an increase in impervious surfaces in the area (MWANGI et al. 2018). Rapid urban developments have occurred with wooded grasslands replaced with concrete structures. This has led to an increase in minimum and maximum temperatures of 1.6 °C and 3.65 °C respectively between 1987 and 2017 ((MWANGI et al. 2018).

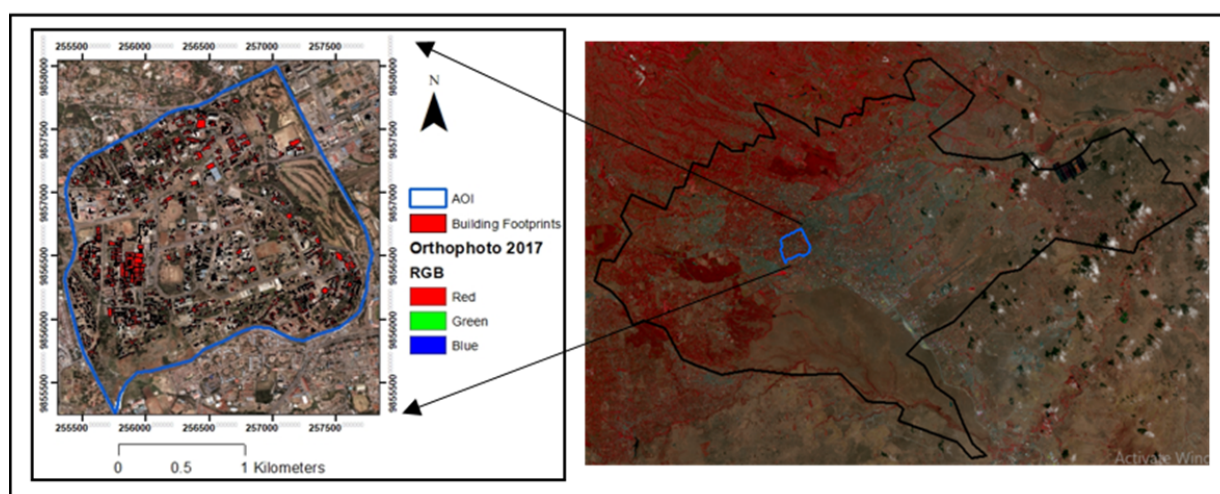


Fig. 1: Location of UpperHill in Nairobi County, Kenya

3 Data processing and methods

Digital topological datasets developed from the stereo imagery acquired in February 1998 were obtained from Survey of Kenya (SoK), which is the national mapping agency in Kenya, at a scale of 1:2500. Landsat LIT imagery, at 30 meter spatial resolution, acquired on 21st February 2000 Landsat 7 sensor was downloaded from the USGS website. There were no thermal data products available during the year which the stereo-aerial imagery was acquired. All data was

processed at UTM, Arc1960 Zone 37 South projection. Figure 2 below gives a summary of the data processes performed on the data.

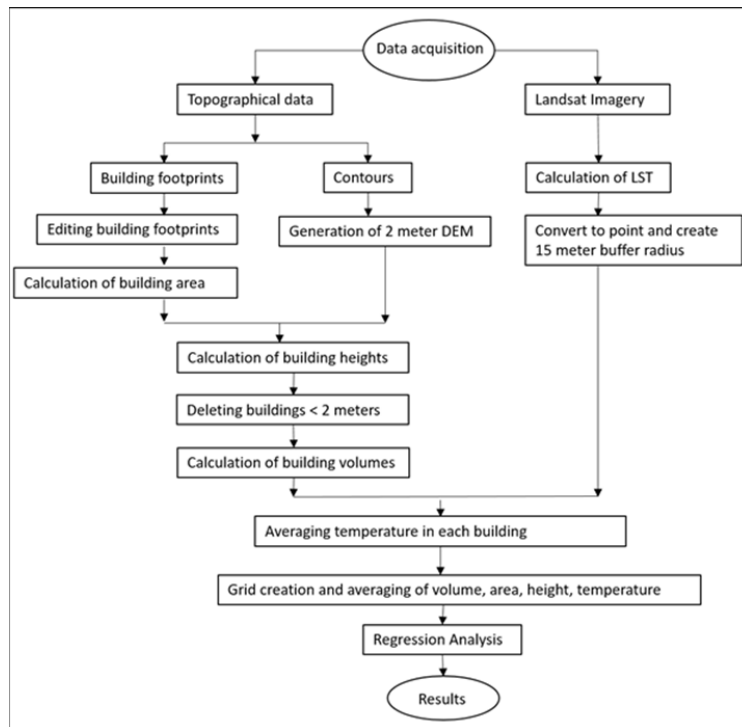


Fig. 2: Methodology framework for topographical datasets and LST

3.1 Editing and Validation of DEM and Building Footprints

Building footprints were extracted from the polygon dataset which also contained other feature classes that were not related to building footprints. Digital stereo-imagery acquired in February 2017 by Ramani Geosystems, Kenya was processed and the orthophoto used a background image in editing the buildings which were still observable from the time of acquisition of the aerial image as shown in figure 3.

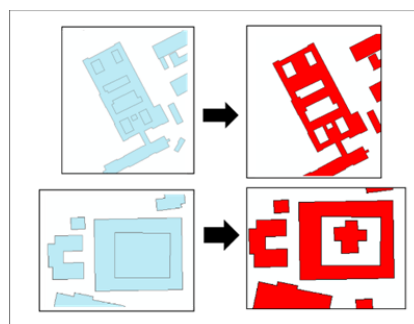


Fig. 3: Edited building footprints using orthophoto as background image

3.1.1 Accuracy of DEM

A DEM at a spatial resolution of 2 meters was generated from the contours dataset from the 1998 topographical data, which had an interval of 2 meters. A value that is calculated to determine DEM accuracy is the root mean square error (RMSE).

$$\text{RMSE} = \sqrt{\frac{\sum_i^m (X_i - X_j)^2}{m-1}} \quad (1)$$

Where X_i is the DEM cell value and X_j is the corresponding sample point elevation, m is the number of sample points.

The accuracy of the interpolated DEM was assessed using GCP points collected in 2017 in areas that had not changed from 1998. An RMSE of 0.23 meters was obtained using equation (1). This accuracy shows how accurately the generated DEM represents the ground truth (Guo-an *et al.*, 2001).

The building dataset had attribute elevation data which enabled the calculation of building heights as the difference between the building elevation and the DEM. Buildings whose height was less than 2 meters were deleted, hence having 1348 building footprints as the final dataset for analysis. Building area was automatically calculated in ArcGIS and verification done manually. Building volume for each building was calculated as the product between the area and its height in ArcGIS 10.4.

3.1.2 Accuracy of Buildings

Since we were not able to measure the building heights to verify the accuracy of the building footprints, data was obtained from internet sources from (<http://www.emporis.com/en/wm/ci/bu/?id=100051>, visit: 23.01.2018). This was in regards to buildings that are still existing in the study area. Floor height was also used to determine the approximate height of the building since building height information is not freely available in this study area. Only three buildings whose data was available from the internet were used to verify as shown in table 1.

Tab. 1: Comparison between actual and extracted building heights

Building name	Floors	Actual Height (m)	Extracted Height (m)	Difference
Social security House	28	103	105.19	2.19
Ministry of Transport	13	43	25.90	17.10
Ardhi House	12	36	23.37	12.63

There was an underestimation of building heights especially for the shorter buildings. Without the stereo-aerial photos or reference data it would be difficult to determine whether the error occurred during the digitization process or from processing the stereo-photos. Eckert, (2008) compared DSM extraction of high resolution stereo-satellite imagery using different software and results showed that in each of the software, buildings less than 50 meters had height differences of <10 meters.

3.2 Calculation of Land Surface Temperature

Landsat imagery was used to calculate land surface temperature for the study area using equations published by USGS for processing data acquired from Landsat 7 ETM+ sensor (NASA, 2009). Computations were carried out using spatial modeler in ArcGIS 10.4.

3.2.1 DN Values to Top of Atmosphere (TOA)

Spectral information is in digital number (DN), which has to be converted to reflectance values for analysis. Landsat 7 ETM+ has two thermal bands, 6a and 6b, resampled to 30 meters. Band 6a was used for this analysis due to its low radiance variance. Equation (2) shows the conversion from DN to Top of Atmosphere (TOA) radiometric values.

$$L_{\lambda} = \left(\frac{L_{max} - L_{min}}{Q_{calmax} - Q_{calmin}} \right) * (Q_{cal} - Q_{calmin}) + L_{min} \quad (2)$$

Where,

L_{λ}	spectral radiance
Q_{calmin}	minimum quantized calibrated pixel value in DN
Q_{calmax}	maximum quantized calibrated pixel value in DN
Q_{cal}	DN value of the pixel
L_{min}	minimum radiance detected by the sensor
L_{max}	maximum radiance detected by the sensor

Equation (2) was used to calculate the at-satellite brightness:

$$T_B = K_2 / \ln\left(\frac{K_1}{L_{\lambda}} + 1\right) \quad (3)$$

Where:

T_B	satellite brightness temperature in degrees Celsius
K_1	band specific thermal conversion constant ($K1_CONSTANT_BAND_n$, where n is band 6a)
K_2	is the band specific thermal conversion constant ($K2_CONSTANT_BAND_n$, where n is band 6a)

3.2.2 Emissivity

NDVI was calculated using the spectral radiance values of the red and infra-red (NIR) bands as calculated using equation (2) so as to determine the land surface emissivity (LSE).

$$R_{TOA\lambda} = \frac{\pi L_{\lambda} d^2}{E_{sun\lambda} \sin\theta_{SE}} \quad (4)$$

Where:

R_{TOA}	top of atmosphere (TOA) planetary reflectance for band x and is unitless
π	3.141592654
d	Earth_Sun_distance in astronomical units
$E_{sun\lambda}$	Band specific mean solar exoatmospheric irradiance
θ_{SE}	Sun elevation angle in degrees from the metadata

NDVI was then calculated using the resulting calculated reflectance values from equation (4) of the red and infra-red bands using equation (5).

$$NDVI = \frac{NIR-R}{NIR+R} \quad (5)$$

Equation (8) calculates the vegetation portion to obtain the LSE as shown in equation (6).

$$P_v = \left(\frac{NDVI - NDVI_{min}}{NDVI_{max} + NDVI_{min}} \right)^2 \quad (6)$$

Where:

P_v	vegetation portion
NDVI	normalized difference vegetation index
$NDVI_{min}$	minimum NDVI
$NDVI_{max}$	maximum NDVI

where the minimum NDVI is the value for pure soil normally given as 0.2 and maximum NDVI is the value of pure vegetation given as 0.5.

LSE is then computed using equation (7):

$$LSE = 0.004 * P_v + 0.986 \quad (7)$$

3.2.3 Land surface temperature

Using the at-satellite brightness temperature and the Land Surface Emissivity, LST was computed in degrees Celsius as shown in equation (8).

$$LST = [T_B / (1 + (\lambda * \frac{T_B}{\rho}) * \ln(LSE))] - 273.15 \quad (8)$$

Where:

LST	land surface temperature
T_B	at-satellite brightness temperature
λ	wavelength of emitted radiance ($\lambda=11.5\mu\text{m}$)
ρ	$h*c/\sigma$ ($1.438*10^{-2}$ m K)
σ	Bolzmenn's constant ($1.38 * 10^{-23}$ J K-1)
h	Planck's constant ($6.26 * 10^{-34}$ J s)
c	velocity of light ($2.998 * 10^8$ m s-1)

Figure 4 below shows the calculated LST around the study area. Areas with lower temperatures have denser vegetation compared to other parts of the study area.

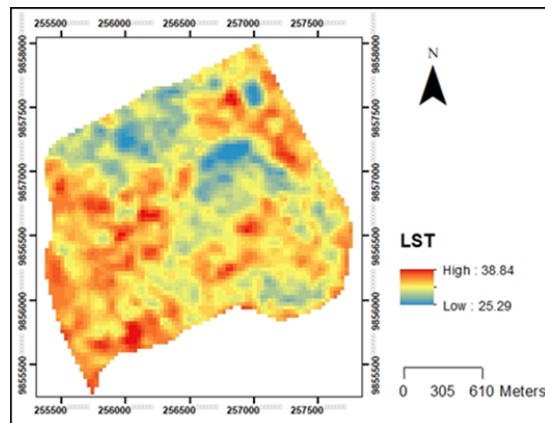


Fig. 4: Calculated LST

3.3 Calculation of Aggregate values

Land surface temperature raster dataset was converted to vector point data, where a 15 meter buffer around each point was created. Spatial analysis was performed between LST polygons and the building data, where a mean LST value was calculated for each building. Summary statistics for the dataset of buildings >2 meters' height are as shown in table 2.

Tab. 2: Summary statistics of elevation, building height, area and volume

	Minimum	Maximum	Mean
DEM Elevation (m)	1663.09	1735.95	1708.27
LST (°C)	26.27	37.70	32.32
Height (m)	2.00	105.19	5.26
Area (m²)	4.16	8570.08	261.76
Volume (m³)	12.64	185483.42	2288.35

A polygon grid of cells 180 meters by 180 meters was created within the study area. This is because of the distribution and size of buildings especially in the center of the study area. 121 grid cells were created each having averaged values of LST, building volumes, area and height of buildings located in each cell, as shown in figure 5.

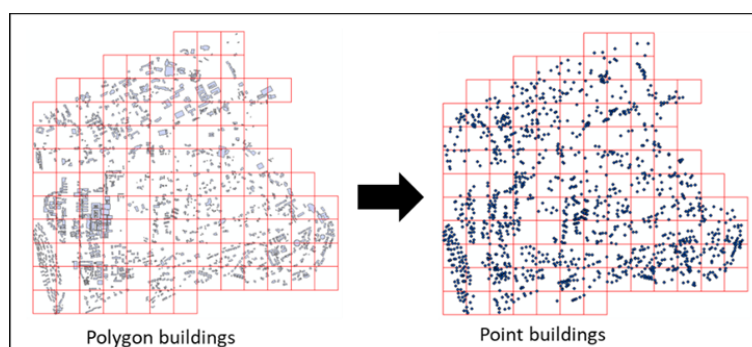


Fig. 5: Building footprints in 180 meter × 180 meter grid cells

4 Results and Discussion

A spatial distribution of the datasets within the grid is as shown in figure 6. Visual inspection in the lower left corner of the study area indicates that areas that had the highest temperatures recorded lower building volume and area. Higher volumes were towards the north western parts of the study area. Areas that have the lower heights, towards the lower right have higher temperatures compared to areas with higher buildings on the northern parts of the study area as in figure 6 (c). The minimum and maximum temperature range within the study area using the averaged values from the buildings was 27.67 °C and 35.40 °C respectively. This was comparatively lower than the minimum and maximum temperature which was 28.02 °C and 35.60 °C respectively, within the grid cells of the LST raster data without averaging the building dataset.

From figure 5, buildings tend to be more clustered towards the lower left. These buildings as well as those on the northern part of the study area have greater volumes as they are large commercial buildings. However, the northern part is highly vegetated compared to the other parts of the study area, which could explain the lower temperatures despite having higher density of buildings.

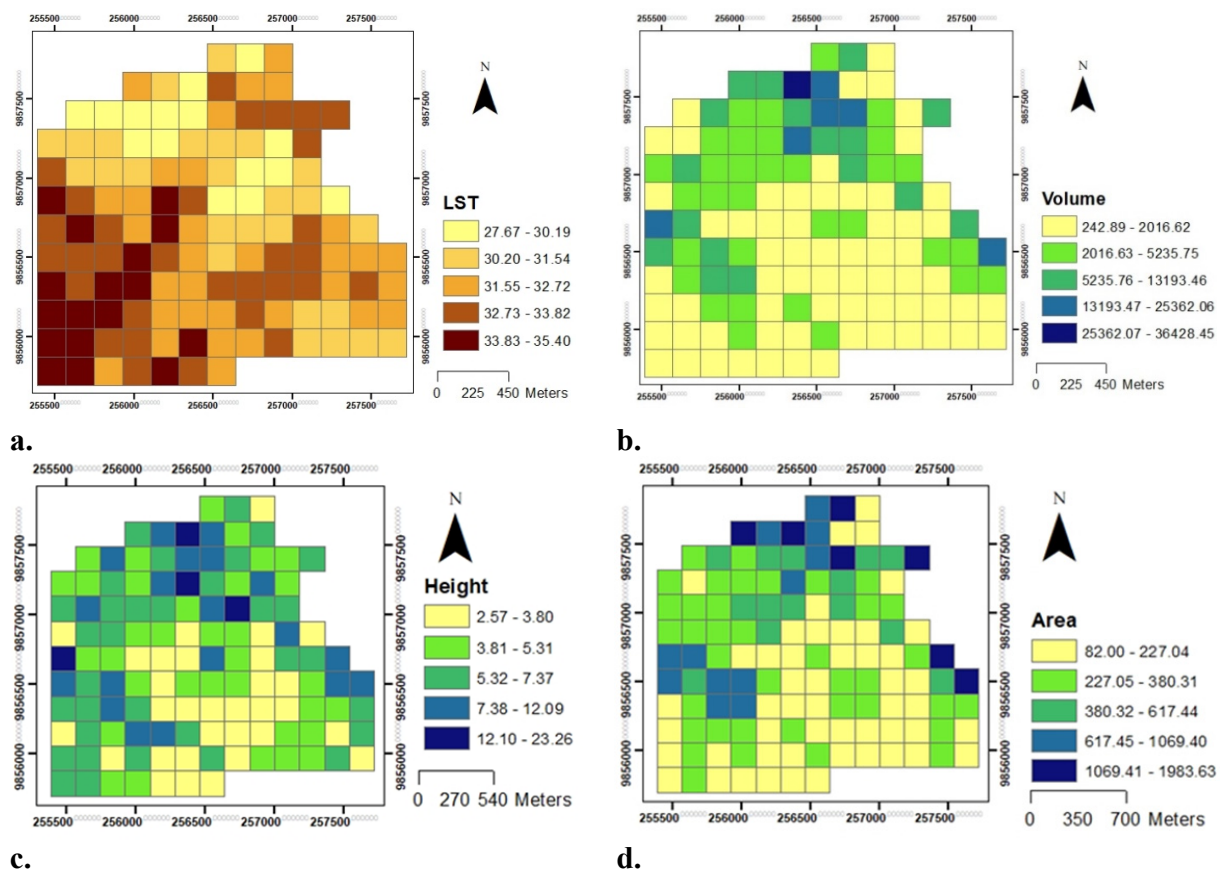


Fig. 6: Spatial distribution of LST (a), building volume (b), area (c) and height (d) in the grid

A linear regression analysis was undertaken on this dataset comprising of 121 spatially averaged building datasets from the grid. Results in figure 7 below show a negative correlation between land surface temperature with volume, area and height. The reliability of the model to predict LST using area, height and volume from the R^2 value indicate that they are not strong predictors, especially area, as also shown in figure 7 (b). This would indicate that there are other factors that affect these data sets such as vegetation density which would need to be considered.

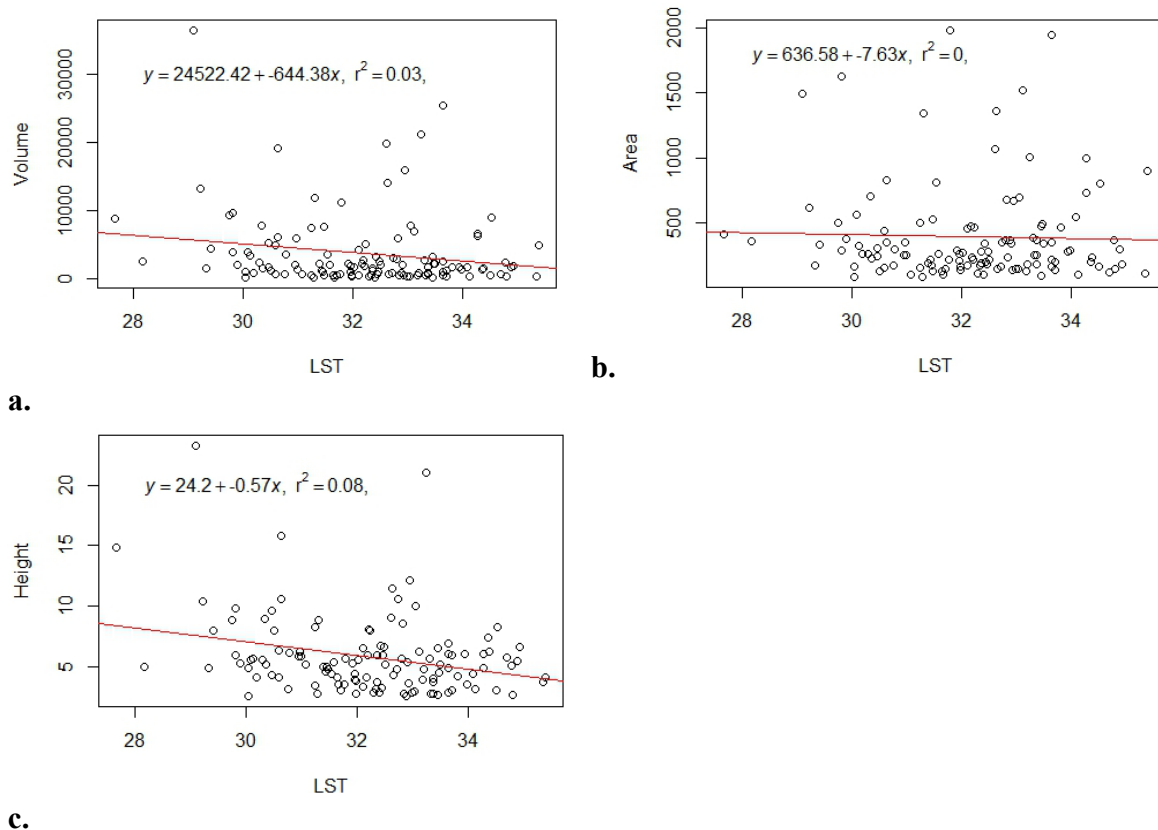


Fig. 7: Regression analysis of land surface analysis with volume (a), area (b), height (c)

5 Conclusion

Quantitative height accuracy and building shape is very important in deriving volumes of buildings for purposes of determining building energy requirements or for planning purposes. This is from the large difference in building heights between the actual building height and those obtained from the digitized buildings. This may have had influence in the results of the analysis. Results show that building height would be a stronger predictor for land surface temperature. Results show that the influence of building volumes on land surface temperature is not significant and cannot be solely explained by buildings. Other factors would need to be taken into consideration such as vegetation density within the study area. Thermal remote sensing dataset from Landsat L1T data products have been resampled to 30 meters hence analysis on individual buildings can be undertaken in areas where higher resolution imagery is not available. Future work will involve comparison of results using time-series data.

6 References

- ALOBEID, A. 2011: Assessment for Matching Algorithms for Urban DSM Generation from Very High Resolution Satellite Stereo Images. Fachrichtung Geodäsie und Geoinformatik der Leibniz University Hanover.
- ALOBEID, A., JACOBSEN, K. & HEIPKE, C., 2009: Building height estimation in urban areas from very high resolution satellite stereo images. ISPRS Hannover Workshop, **5**, 2-5.
- ECKERT, S., 2008: 3D-Building Height Extraction from Stereo IKONOS Data Quantitative and Qualitative Validation of Digital Surface Models Derivation of Building Height and Building Outlines.
- EL GAROUANI, A., ALOBEID, A. & EL GAROUANI, S., 2014: Digital surface model based on aerial image stereo pairs for 3D building. International Journal of Sustainable Built Environment, **3**(1), 119-126.
- GUO-AN, T.A.N.G., STROBL, J., JIAN-YA, G.O.N.G., MU-DAN, Z.H.A.O. & ZHEN-JIANG, C., 2001: Evaluation on the accuracy of digital elevation models. Journal of Geographical Sciences, **11**(2), 209-216.
- MWANGI, P.W., KARANJA, F.N. & KAMAU, P.K., 2018: Analysis of the Relationship between Land Surface Temperature and Vegetation and Built-Up Indices in Upper-Hill, Nairobi. Journal of Geoscience and Environment Protection, **6**(1), 1-16.
- NASA. 2009: Landsat 7 science data users handbook. National Aeronautics and Space Administration Landsat, 186.
- WU, C.D., LUNG, S.C.C. & JAN, J.F., 2013: Development of a 3-D urbanization index using digital terrain models for surface urban heat island effects. ISPRS Journal of Photogrammetry and Remote Sensing, **81**, 1-11.
- ZHAO, Q., MYINT, S.W., WENTZ, E.A. & FAN, C., 2015: Rooftop surface temperature analysis in an urban residential environment. Remote Sensing, **7**(9), 12135-12159.